Applied Surface Science 272 (2013) 119–123

Contents lists available at SciVerse ScienceDirect

Applied Surface Science

journal homepage: www.elsevier.com/locate/apsusc

X-ray emission analysis of a plasma source using an yttrium and a mylar target for the generation of 2.48 nm wavelength microbeam

Libero Palladino[a,b], Ramon Gimenez De Lorenzo[a,b], Maurizio Di Paolo Emilio[a,b], Tania Limongi[c,*]

[a] Dipartimento di Fisica, Universita' de L'Aquila, Italy
[b] INFN, Laboratorio Nazionale del Gran Sasso, Assergi (AQ), Italy
[c] Istituto Italiano di Tecnologia (IIT), Via Morego 30, 16163 Genova, Italy

ARTICLE INFO

Article history:
Available online 17 October 2012

Keywords:
X-ray microbeam
Plasma source

ABSTRACT

In this work, the characteristics of X-ray beam generated from a plasma produced by focusing a Nd-Yag/glass laser beam on mylar or yttrium target were presented.

For each target material, the conversion efficiencies of the soft X-ray emission in two different energy ranges, (i) 300–510 eV (almost coincident with the Water Window), (ii) 450–850 eV were measured. The experimental results of the conversion efficiencies will be utilized at the PLASMA-X laboratory of L'Aquila University for the realization of an intense monochromatic X-ray microbeam to be used in radiobiological and in transmission X-ray microscopy applications. In the presented experimental set-up, at the wavelength of 2.48 nm, a monochromatic soft X-rays beam was collected by multilayer spherical mirrors reflecting at an incidence angle close to the normal of the surface.

The optical system geometry, the monochromatic beam intensity and the measures of efficiency of conversion of X-ray were described in this paper [5].

1. Introduction

In last years, the X-ray micro-beam are becoming important experimental tools in the field of radiobiology and for the imaging of biological samples. Microbeams have contributed significantly to the discovery and characterization of new findings regarding the interaction process of the ionizing radiation with cells and tissues. Using an X-ray microbeam single cell approach, it has been possible to study also different implications, such as apoptosis, of the bystander effect where radiation damage is expressed in cells which have not been directly irradiated but were in contact or shared media with directly exposed samples [7]. In the field of radiobiology, is now thought necessary to investigate the biological effects of ionizing radiation at low doses and low energy photons (100 eV to 1.5 keV).

The microscopic size of the beam at the point of focus allows both to irradiate the cells or parts thereof such as DNA and that can be used in the develop a transmission X-ray microscopy apparatus [2–5].

The great interest in the development of X-ray microbeam is definitely due to the high spatial resolution achievable; to focus a X-ray beam, the optics, which is currently used, are the zone plates. They have a low efficiency of transmission of radiation, only a few percent, and with a collecting area of the radiation of about 10 mm in diameter [9,8]. These features make the zone plate suitable in synchrotron light sources applications, but poorly adapted to the plasma sources. In fact, with the synchrotron light sources intense and monochromatic radiation compensated for the low efficiency of the zone plates use in the optical layout. While with a laser-plasma source, due to an average low X-ray emission on a 2π sr solid angle, the use of zone plates, as focusing lenses, will not be suitable.

Recently, spherical mirrors for soft X-rays reflecting at an incidence angle close to the normal, have been developed. They can be characterized with a large collecting area and with a reflectivity of between 30% and 1% with an $\lambda/\Delta\lambda \approx 200$ (depends on the used X-ray wavelength) [1].

2. Experimental apparatus

A laser-plasma source with the interaction chamber at 10^{-3} mbar internal pressure was used at the PLASMA-X laboratory of L'Aquila University. The Nd YAG/glass laser generated a pulse of 6 ns long and with an energy which depends on three operating configurations: about 300 mJ, about 1.5 and about 4 J.

The focal spot size was 65 ($\pm$2) μm, which corresponded to a power density between 10^{12} and 10^{13} W/cm^2. The X-rays were

* Corresponding author at: Istituto Italiano di Tecnologia (IIT), Via Morego 30, 16163 Genova, Italy.
E-mail address: tania.limongi@gmail.com (T. Limongi).

0169-4332/$ – see front matter © 2012 Elsevier B.V. All rights reserved.
http://dx.doi.org/10.1016/j.apsusc.2012.09.097

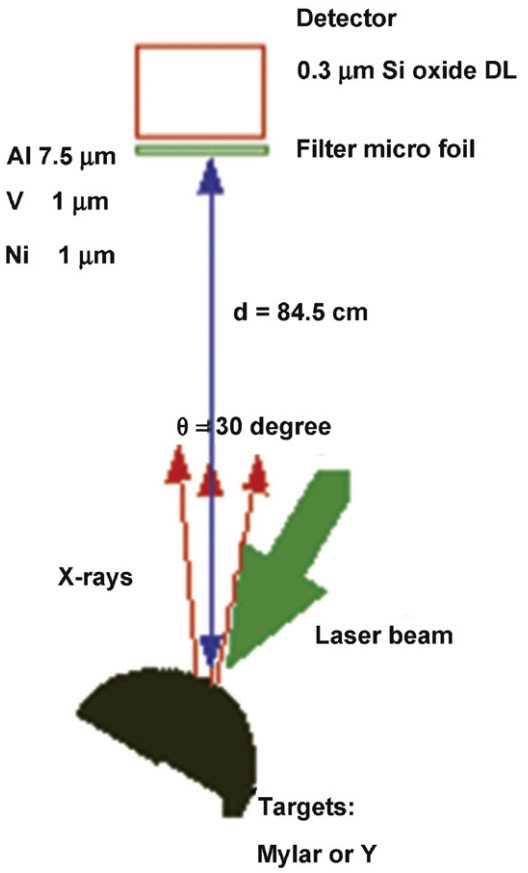

Fig. 1. Schematic description of the experimental arrangement for the conversion efficiency measurement. The geometrical parameters of the measure are shown in the figure.

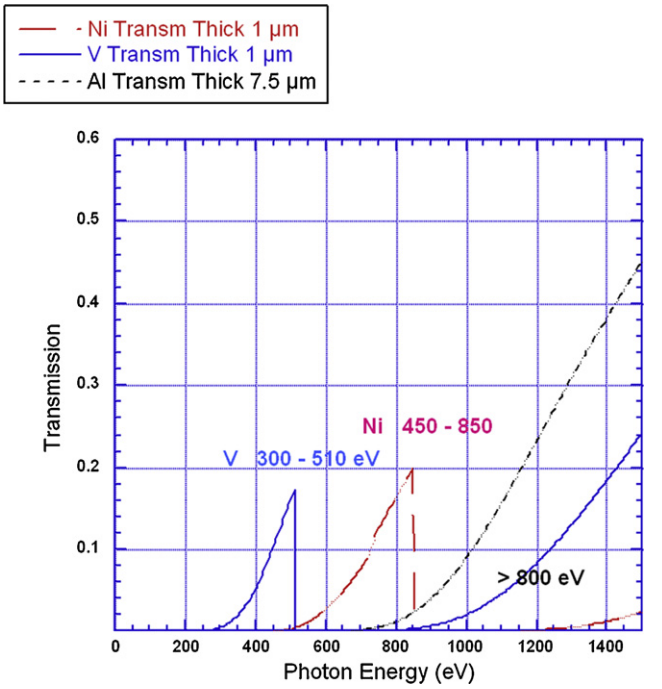

Fig. 2. Transmission curves for the three microfoils used. The vanadium microfoil, 1 μm tick, has a average transmission ≈ 10% between 300 and 510 eV and a tail to higher energy of 800 eV. The nickel microfoil, 1 μm tick, has a average transmission ≈ 12% between 500 and 800 eV and a small tail to higher energy of 800 eV. The aluminum microfoil, 7.5 μm tick, has a significant transmission for energies greater than 800 eV.

detected using a PIN-diode (100-PIN-125, with SiO_2 0.3 μm as entrance window, dead layer, and Si 125 μm as intrinsic zone, by Emerge Corporation).

The detector was placed at a 30° angle in direction of the laser beam with a 7 mm diameter sensitive area. A second detector was to measure the X-ray intensity to provide the focus on the target with the best conditions. This detector had an aluminum micro-foil 3 μm thick entrance window and was placed at 60° with respect to the direction of the laser beam.

To make measures of X-ray conversion efficiency of mylar and yttrium, the pin diode was placed at a distance of 84.5 cm from plasma. The radiation was filtered by putting in front of the detector entrance window either a vanadium microfoil 1 μm tick or a nickel microfoil 1 μm tick or an aluminum microfoil 7.5 μm. Fig. 1 shows the schematic experimental set-up and indicates the geometrical parameters and the characteristics of the microfoils used as X-ray filters. The spherical mirror holder and the target are controlled by computer.

The 2.48 nm monochromatic microbeam is obtained by using a multilayer spherical mirror which selects the wavelength of X-rays at an 8° incident angle from the normal of the mirror. The mirror has a useful diameter $D = 30$ mm and a curvature radius $R = 265$ mm.

A membrane of 50 nm thick silicon nitride protected the mirror from the debris produced during the formation of the plasma.

The sensitivity of the movement is 1 μm.

This mechanical configuration will be used in future to obtain monochromatic micro-beams with different optical configurations and various X-ray energies.

3. Experimental results

3.1. Measurement of conversion efficiencies

To measure the conversion efficiency in the range of about 300–510 eV and between about 450 and 800 eV, a 1 μm tick vanadium microfoil and a 1 μm tick nickel microfoil were placed in front of entrance window of the detector respectively. For the measurement of the radiation component of more than 800 eV, we used an 7.5 μm thick aluminum microfoil.

In Fig. 2 the transmission curves for the three microfoils used were reported. The vanadium microfoil 1 μm tick had a transmission range between 300 and 510 eV with a tail to higher energy of 800 eV. The nickel microfoil 1 μm tick had a transmission between 500 and 800 eV with a tail to higher energy of 800 eV, but less important than that of vanadium. Instead, the aluminum microfoil of 7.5 μm tick had a significant transmission for energies greater than 800 eV [6].

To obtain the conversion efficiency from the experimental data for the intervals between about 300 and 510 eV (V) and between 450 and 850 eV (Ni) was necessary to subtract the contribution of photons with energy greater than 800 eV from the total signal of the detector filtered with the V and Ni. This contribution was derived from the detector signals filtered with 7.5 μm of aluminum, which as shown in Fig. 2 has a transmission ($>10^{-4}$) for photon energy greater than 800 eV.

For a given material used as a target, the shape of the distribution of the intensity of X-rays as a function of energy, $S(E_x)$, is almost the same if for each pulse of the laser are realized the same experimental conditions. That is if the duration of the laser pulse, the energy per pulse and the power density are approximately equal, within statistical fluctuations.

Since the data obtained with the three filters (V, Ni and Al) were collected under the same conditions of laser pulse energy and

Table 1
Analysis of the X-rays intensity measurements, mylar and yttrium conversion efficiencies (on 2π sr) for the three energy intervals indicated in the table for $E_{laser} \approx 300$ mJ.

W (W/cm^2)	Filter	Energy interval (eV)	E_x (mJ in 2π sr)	η% (in 2π sr)
Target MYLAR – $E_{laser} = 321 \pm 7$ mJ				
1.4×10^{12}	V 1 μm tick	300–510	3.93	1.2
1.4×10^{12}	Ni 1 μm tick	450–850	1.34	0.4
1.4×10^{12}	Al 7.5 μm tick	>800 eV	2 μJ in 2π sr	6×10^{-4}
Target Y – $E_{laser} = 308 \pm 9$ mJ				
1.3×10^{12}	V 1 μm tick	300–510	10.2	3.3
1.3×10^{12}	Ni 1 μm tick	450–850	1.4	0.5
1.3×10^{12}	Al 7.5 μm tick	>800 eV	9.8 μJ in 2π sr	3×10^{-3}

Table 2
Analysis of the X-rays intensity measurements, mylar and yttrium conversion efficiencies (on 2π sr) for the three energy intervals indicated in the table for $E_{laser} \approx 1.6$ J.

W (W/cm^2)	Filter	Energy interval (eV)	E_x (mJ in 2π sr)	η% (in 2π sr)
Target MYLAR – $E_{laser} = 1.6 \pm 0.1$ J				
6.9×10^{12}	V 1 μm tick	300–510	59.1	3.7
6.9×10^{12}	Ni 1 μm tick	450–850	22.9	1.4
6.9×10^{12}	Al 7.5 μm tick	>800 eV	0.3	2×10^{-2}
Target Y – $E_{laser} = 1.63 \pm 0.06$ J				
7×10^{12}	V 1 μm tick	300–510	136.8	8.4
7×10^{12}	Ni 1 μm tick	450–850	22.4	1.4
7×10^{12}	Al 7.5 μm tick	>800 eV	0.35	2×10^{-2}

power density on target, we assume that the distribution of intensity of X-ray emission from plasma can be considered similar for each of three laser energy situations.

Thus, for a given target, there follow three relations:

$$Q_V^{tot} \propto \int S(E_x) \cdot T_{DL}(E_x) \cdot T_V^{t=1\ \mu m}(E_x)\, dE_x \quad (1)$$

$$Q_{Ni}^{tot} \propto \int S(E_x) \cdot T_{DL}(E_x) \cdot T_{Ni}^{t=1\ \mu m}(E_x)\, dE_x \quad (2)$$

$$Q_{Al}^{tot} \propto \int S(E_x) \cdot T_{DL}(E_x) \cdot T_{Al}^{t=7.5\ \mu m}(E_x)\, dE_x \quad (3)$$

where Q_V^{tot}, Q_{Ni}^{tot} and Q_{Al}^{tot} charges are the integrated signal of the detector filtered with V, Ni and Al, respectively. $T_{DL}(E_x)$, $T_V^{t=1\ \mu m}(E_x)$, $T_{Ni}^{t=1\ \mu m}(E_x)$ and $T_{Al}^{t=7.5\ \mu m}(E_x)$ are the transmissions, versus X-ray energy, E_x, of the dead layer detector and the V, Ni and Al microfoils respectively.

The proportionality factors in the relations (1), (2) and (3), were considered constant because the geometrical and physical conditions of the measures remain unchanged, as shown in Fig. 1.

In our experimental conditions, the total charge, Q_{Al}^{tot}, measured by the PIN diode, mainly depends from the charge contribution, $Q_{Al}^{E_x>800\,eV}$, of the spectral region characterized by a photon energy greater than 800–850 eV. In fact, in this region, the 7.5 μm Al filter's transmission (transmission > 10^{-4}) becomes significant and then we can approximate $Q_{Al}^{tot} \approx Q_{Al}^{E_x>800\,eV}$.

Consequently we can write for vanadium

$$\frac{Q_V^{E_x>800\,eV}}{Q_{Al}^{tot}} \approx \frac{\int_{800\,eV} S(E_x) \cdot T_{DL}(E_x) \cdot T_V^{t=1\ \mu m}(E_x)\, dE_x}{\int_{800\,eV} S(E_x) \cdot T_{DL}(E_x) \cdot T_{Al}^{t=7.5\ \mu m}(E_x)\, dE_x} \approx \frac{\int_{800\,eV} T_V^{t=1\ \mu m}(E_x)\, dE_x}{\int_{800\,eV} T_{Al}^{t=7.5\ \mu m}(E_x)\, dE_x}$$

the product $S(E_x) \times T_{DL}$ give about the same contribution to the integral value and the charge ratio depends principally from the filter transmission.

So also for nickel we can write:

$$\frac{Q_{Ni}^{E_x>850\,eV}}{Q_{Al}^{tot}} \approx \frac{\int_{850\,eV} S(E_x) \cdot T_{DL}(E_x) \cdot T_{Ni}^{t=1\ \mu m}(E_x)\, dE_x}{\int_{850\,eV} S(E_x) \cdot T_{DL}(E_x) \cdot T_{Al}^{t=7.5\ \mu m}(E_x)\, dE_x} \approx \frac{\int_{850\,eV} T_{Ni}^{t=1\ \mu m}(E_x)\, dE_x}{\int_{850\,eV} T_{Al}^{t=7.5\ \mu m}(E_x)\, dE_x}$$

where $Q_V^{E_x>800\,eV}$ and $Q_{Ni}^{E_x>850\,eV}$ are the charges of the integrated detector signals filtered with V and Ni for X-ray energy greater than 800 eV and 850 eV, respectively.

From previous assumptions, the signal component for energies greater than 800 eV is given by

$$Q_V^{E_x>800\,eV} \approx Q_{Al}^{tot} \cdot \frac{\int_{800\,eV} T_V^{t=1\ \mu m}(E_x)\, dE_x}{\int_{800\,eV} T_{Al}^{t=7.5\ \mu m}(E_x)\, dE_x} \quad (4)$$

$$Q_{Ni}^{E_x>850\,eV} \approx Q_{Al}^{tot} \cdot \frac{\int_{850\,eV} T_{Ni}^{t=1\ \mu m}(E_x)\, dE_x}{\int_{850\,eV} T_{Al}^{t=7.5\ \mu m}(E_x)\, dE_x} \quad (5)$$

Table 3
Analysis of the X-rays intensity measurements, mylar and yttrium conversion efficiencies (on 2π sr) for the three energy intervals indicated in the table for $E_{laser} \approx 3.7$ J.

W (W/cm^2)	Filter	Energy interval (eV)	E_x (mJ in 2π sr)	η% (in 2π sr)
Target MYLAR – $E_{laser} = 3.7 \pm 0.2$ J				
1.6×10^{13}	V 1 μm tick	300–510	146.6	4.0
1.6×10^{13}	Ni 1 μm tick	450–850	83.6	2.3
1.6×10^{13}	Al 7.5 μm tick	>800 eV	1.2	3×10^{-2}
Target Y – $E_{laser} = 3.7 \pm 0.2$ J				
1.6×10^{13}	V 1 μm tick	300–510	413.4	11.2
1.6×10^{13}	Ni 1 μm tick	500–850	67.2	1.8
1.6×10^{13}	Al 7.5 μm tick	>800 eV	1.6	4×10^{-2}

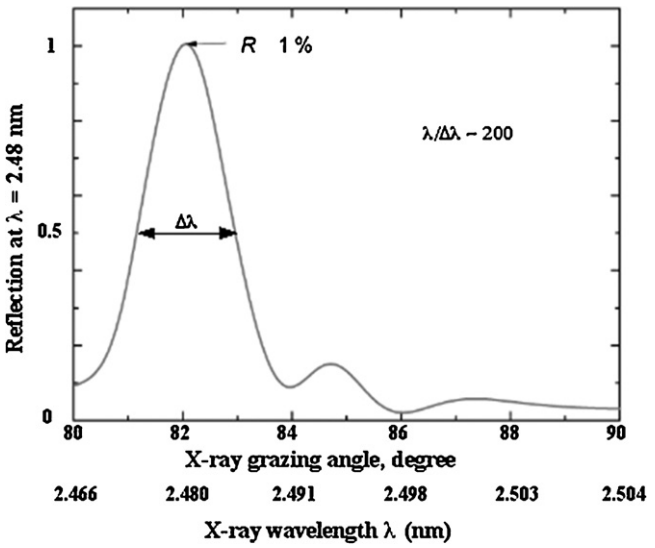

Fig. 3. Curve of the reflectivity of the multilayer deposited on the substrate of the sherical mirror. It has a reflectivity of about 1% for Bragg angle of 82° which corresponds to a photon energy of 500 eV.

Subtracting (1) from (4) and (2) from (5), the X-ray signals from the windows of the V (300–510 eV) and Ni (450–850 eV) was obtained by the following relations

$$Q_{\mathrm{V}}^{300-510\,\mathrm{eV}} = Q_{\mathrm{V}}^{\mathrm{tot}} - Q_{\mathrm{V}}^{E_{\mathrm{X}}>800\,\mathrm{eV}} \quad (6)$$

$$Q_{\mathrm{Ni}}^{450-850\,\mathrm{eV}} = Q_{\mathrm{Ni}}^{\mathrm{tot}} - Q_{\mathrm{Ni}}^{E_{\mathrm{X}}>850\,\mathrm{eV}} \quad (7)$$

In the previous equations, we have assumed a uniform distribution of the X-ray intensity inside of the two energy ranges. Using (6) and (7) equations in the experimental data analysis for the yttrium and mylar were shown in Tables 1–3 for the three configurations of the laser energy. The energy of the laser beam were indicated in each tables. In these tables for each target material, the power density on the target and the X-ray energy produced by the plasma with the conversion efficiencies for the 3 different energy ranges were reported.

3.2. Measurement of microbeam

One of the aims of the presented work is to realize a monochromatic microbeam at 2.48 nm wavelength, which is within the water window energy region.

To reflect and select photons with a wavelength of 2.48 nm, a multilayer spherical mirror [1] with a resolution $\lambda/\Delta\lambda \approx 200$ and a reflectivity ≈ 1% was used. The multilayer structure includes two packets: 230 periods with a step of 1.256 nm and 220 periods with a step of 1.2475 nm. The material in both packets is W/B4C.

The photons were selected with a reflection angle of 8 degrees from the normal of the mirror surface.

In Fig. 3 the reflection curve of the mirror with geometric parameters was shown.

The component to 2.48 nm had been focused in the geometry shown in Fig. 4.

The mirror plasma distance was 201.5 mm and the image point of the plasma was formed at a distance of 400.2 mm from the mirror.

The X-ray detector was placed in the proximity of the focus point of the monochromatic beam.

A vanadium microfoil 1 micron thick was placed before the input of a detector to separate the ultraviolet and visible window. The soft X-rays were generated from an yttrium target with a laser beam energy of 3.6 J.

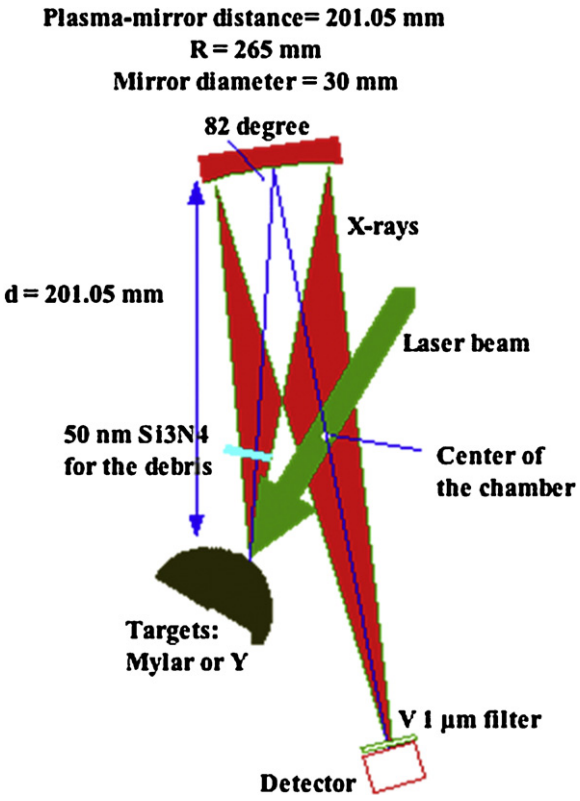

Fig. 4. Schematic description of the experimental microbeam arrangement for the measurement of the energy of the X-ray beam reflected from the sherical mirror. The figure shows the optical configuration of the microbeam.

The charge collected by the detector was 4 nC which corresponding approximately to 3×10^9 photons of 500 eV energy. Considering the magnification 2 of the image of the source the focus of micriobean can be estimated having a density of photons equal to 2×10^5 fotoni/μm^2.

4. Conclusions and discussion

From the experimental data, in the vanadium energy window, which almost coincide with the water window, yttrium conversion efficiency was systematically 2 or 3 times larger than mylar conversion efficiency, whereas, in the nickel energy window, the two materials performed conversion efficiencies essentially identical. This happens with every power density.

The difference in vanadium energy window is due to the type of spectrum emitted by the two materials. Yttrium produced a quasi-continuous emission due to the threshold M that was excited and a uniform spectrum around 400 eV. Instead, the mylar generated a line spectrum of the carbon K threshold (280 eV). The conversion efficiencies were similar for the two materials in the energy region of the nickel window, because they mainly emit bremsstrahlung radiation. In the Water Window, yttrium presents a good X-ray emitter and can be employed in X-ray microscopy where an image of a biological sample with a single X-ray shot has to be obtained.

The micro-beam measures show that 3×10^9 photons of 500 eV energy correspond approximately to a photon density of 2×10^5 photon/line/μm^2. This value is according to that obtained from similar LPS as the source realized by Jansson et al. [3] in which the authors employ the liquid nitrogen as target.

This result is of considerable interest for applications in biology.

In this article we have presented the preliminary results of X-ray reflected from the mirror.

In future it is planned measures and analysis of the optical characteristics of the microbeam using a new mechanical layout.

Moreover, a future program will be of analyze the X-ray emissions using other materials as rhenium.

Acknowledgments

We would like to thank Dott. L. Votano Director of Gran Sasso National Laboratories of INFN and Prof. S. Santucci Director of the Physics Department of L'Aquila University for supporting us. This work is financially supported by INFN, PLAXA experiment.

References

[1] I. Artyukov, Y. Bugayev, et al., X-ray Schwarzschild objective for the carbon window (lambda similar to 4. 5 nm), Opt. Lett. 34 (19) (2009) 2930–2932.
[2] S. Gerardi, Ionizing radiation microbeam facilities for radiobiological studies in Europe, J. Radiat. Res. (Tokyo) 50 (2009) A13–A20.
[3] P.A.C. Jansson, U. Vogt, et al., Liquid-nitrogen-jet laser-plasma source for compact soft X-ray microscopy, Rev. Sci. Instrum. 76 (4) (2005).
[4] Y. Kobayashi, T. Funayama, et al., Microbeam irradiation facilities for radiobiology in Japan and China, J. Radiat. Res. (Tokyo) 50 (Suppl. A) (2009) A29–A47.
[5] J.A. Koch, O.L. Landen, et al., High-energy X-ray microscopy techniques for laser-fusion plasma research at the National Ignition Facility, Appl. Opt. 37 (10) (1998) 1784–1795.
[6] L.B.N. Laboratory, X-ray Data Booklet Center for X-ray Optics and Advanced Light Source.
[7] K.M. Prise, G. Schettino, et al., Microbeam Studies of the Bystander Response, J. Radiat. Res. (Tokyo) 50 (2009) A1–A6.
[8] G. Schmahl, B. Niemann, et al., X-ray microscopy – experimental results with the Gottingen X-ray microscope at the electron storage ring bessy in Berlin, J. Microsc. Oxford 138 (June) (1985) 279–284.
[9] G. Schmahl, D. Rudolph, et al., Zone-plate X-ray microscopy, Q. Rev. Biophys. 13 (3) (1980) 297–315.